Finite Element Analysis of Stress Evolution at Metal-Oxide Interface during High Temperature Oxidation

Jaeheon Kim [a], Chi Bum Bahn [a]*
[a]School of Mechanical Engineering, Pusan National Univ., Busan, 46241, South Korea
[*]Corresponding author: bahn@pusan.ac.kr

***Keywords :** Finite Element Anaylsis, Stress Evolution, High Temperature Oxidation, Thermomechanical Model

1. Introduction

Commonly, many alloys maintain their corrosion resistance by adding elements with superior corrosion resistance, such as chromium, silicon, and aluminum. These elements primarily protect alloys from corrosion by forming a stable oxide layer during oxidation. However, in high-temperature environments, maintaining this oxide film becomes challenging. As temperature increases, the growth of the oxide film accelerates, leading to failures such as spallation or cracking due to incompatible mechanical properties between the substrate and oxide film, ultimately reducing corrosion resistance [1]. This phenomenon may significantly affect the lifetime of alloys and structures. Therefore, residual stresses at high temperatures have been extensively studied. However, obtaining in-situ data under these conditions is difficult; thus, many studies rely on experimental data obtained after cooling.

In this study, we conducted simulations to analyze stress evolution at the metal-oxide interface at high temperatures using commercial finite element analysis (FEA) software, Abaqus, which is effective for simulating high-temperature oxidation phenomena through a comprehensive thermomechanical model. To accurately capture stress variations at the interface, we utilized a UMAT (User Material) subroutine, which is invoked during calculations at each spatial location.

2. Theoretical background for thermomechanical modelling

In this section, we present the theoretical foundation for simulating high temperature oxidation that has been used in earlier works [2,3]. The strain composition to implement the model is shown in Fig. 1. Ni30Cr was assumed as alloy materials in this simulation following the earlier work [2].

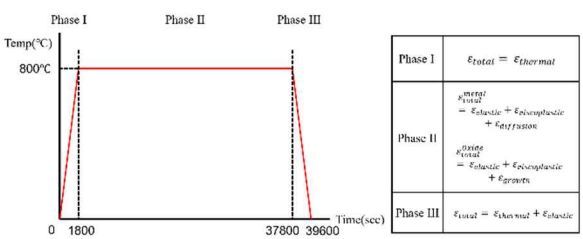

Fig. 1. Strain decomposition by phase

2.1 Elastic strain

The elasticity for isotropic isothermal condition can be described by Hooke's model as in Eq. (1) with Lame' s coefficient λ, and μ:

$$\sigma_{ij} = \lambda\delta_{ij}\,\varepsilon_{kk} + 2\mu\varepsilon_{ij} \tag{1}$$

This can be implemented as Jaumann rate equation by integrating in a corotational framework:

$$\Delta\sigma^{J}_{ij} = \lambda\delta_{ij}\,\Delta\varepsilon_{kk} + 2\mu\Delta\varepsilon_{ij} \tag{2}$$

2.2 Creep strain

A Norton-Hoff power law is used for creep strain:

$$\frac{\varepsilon_{creep}}{dt} = \frac{1}{2}\dot{\varepsilon}n\ \ (\sigma)\left(\frac{|\sigma|}{K}\right)^{N} \tag{3}$$

Where K stands for creep parameter and N is the Norton exponent.

2.3 Thermal strain

Difference between thermal expansion coefficients generates thermal stress during oxidation. For thermal strain, classical thermal equation is being used:

$$\frac{\varepsilon_{therm\,al}}{dt} = \alpha(T)\frac{dT}{dt} \tag{4}$$

Thermal expansion coefficient α should vary with temperature. However, we assume that it is constant due to heating and cooling time relatively short compared to isothermal phase.

2.4 Diffusion strain

As oxidation continues, chrome diffuses from metal to form chrome oxide on the surface. Nevertheless, the diffusion leads to changing lattice spacing that can generate strain especially near the metal surface:

$$\varepsilon_{diffusion}\ \ (z) = \eta([Cr](z,t) - [Cr]_i)\bar{\bar{I}} \tag{5}$$

Where η is constant coefficient coupling the chromium concentration profiles to the diffusion strain. $[Cr](z,t)$ is chromium concentration profiles as

function of z. $[Cr]_i$ is initial chromium concentration. $\bar{\bar{I}}$ is second-rank identity tensor of dimension 3.

2.5 Growth strain

During the oxidation process, we assume that thickness of oxide grows as follows:

$$h_{ox} = A_p\sqrt{t} \tag{6}$$

For oxide growth strain, we consider Clarke relation that has been studied in previous work:

$$\frac{\varepsilon_{growth}}{dt} = D_{ox} * \frac{dh_{ox}}{dt} \tag{7}$$

Where D_{ox} is the parameter for growth strain. D_{ox} is varies with temperature following Arrhenius relation. However, we only consider growth strain in isothermal phase, the temperature dependency can be neglectable.

2.6 Thermomechanical modeling

We assume there are no non-linear mechanical phenomena such as buckling, spallation, etc. Furthermore, two-dimensional behavior is also neglected. With these assumptions, we can possibly prove the continuity of strain. With the proposed strain decomposition, we can propose the relation between metal and oxide that leads to:

$$\left(\frac{\varepsilon_{elastic}}{dt} + \frac{\varepsilon_{creep}}{dt} + \frac{\varepsilon_{thermal}}{dt} + \frac{\varepsilon_{diffusion}}{dt}\right)_m = \left(\frac{\varepsilon_{elastic}}{dt} + \frac{\varepsilon_{creep}}{dt} + \frac{\varepsilon_{thermal}}{dt} + \frac{\varepsilon_{growth}}{dt}\right)_{ox} \tag{8}$$

3. Abaqus Implementation

The simulated geometry is a single 20×20×20 μm cubic part, with the top 2 μm partitioned for oxide, including an air layer. The presence of the air layer is intentionally included as one of the simulation strategies, converting it into oxide properties progressively as oxidation proceeds. Additionally, as shown in Table 1, stress calculation for the air layer is prevented by assigning it an extremely low Young's modulus and Poisson's ratio. The input parameters used in the simulation are listed in Table 1.

.

Table. 1: Input material properties [2,4-6]

Parameter	Metal(Ni30Cr)	Oxide	Air
E (MPa)	170,000	225,000	1E-6
υ	0.3	0.29	0.0
N	1	1	-
K ($MPa^{1/N}$)	2.39E+11	2.65E+8	-
$\alpha(K^{-1})$	1.9E-5	6.99E-6	-
η	-6.75eE-3	-	-

3.1 Phase definition by temperature

As shown in Fig 1, the simulation process consists of three steps. The detailed schematic for model implementation is illustrated in Fig. 2

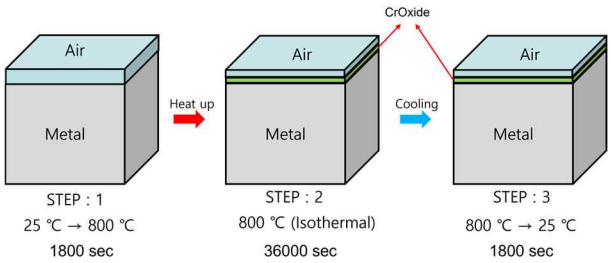

Fig. 2. Schematic of step definition

In phase one, the phase is divided into 10 increments, meaning $\Delta T = 77.5℃$ per increment. We assume the metal has not yet formed an oxide layer; thus, only thermal strain due to metal expansion is considered.

In phase two, spanning from 1,800 to 37,800 seconds, the temperature is maintained at 800℃ for 10 hours, divided into 60 increments. In this phase, the elements initially assigned as the air layer transform into chrome oxide properties as oxide grows according to Eq. (6). Furthermore, as the oxide layer forms, we compute elastic strain, creep strain, diffusion strain, and growth strain. Thermal strain is no longer considered since there is no temperature change during this phase.

In phase three, from 37,800 to 39,600 seconds, we cool the model down to 25℃ over 20 increments. We assume that decreasing temperature results in insufficient activation energy for creep and diffusion, and no further oxide growth occurs. Thus, only elastic strain and thermal strain are considered in this phase.

3.2 UMAT subroutine algorithm

The flowchart for simulation algorithm is shown in Fig. 3. At the start of the UMAT subroutine, variables required for integration with Abaqus software are defined. Following this, variables are initialized to zero.

Each integration point considers two different conditions: one determined by the simulated temperature phase based on simulated time t and the other determined by material properties based on the y-axis coordinates COORDS(2).

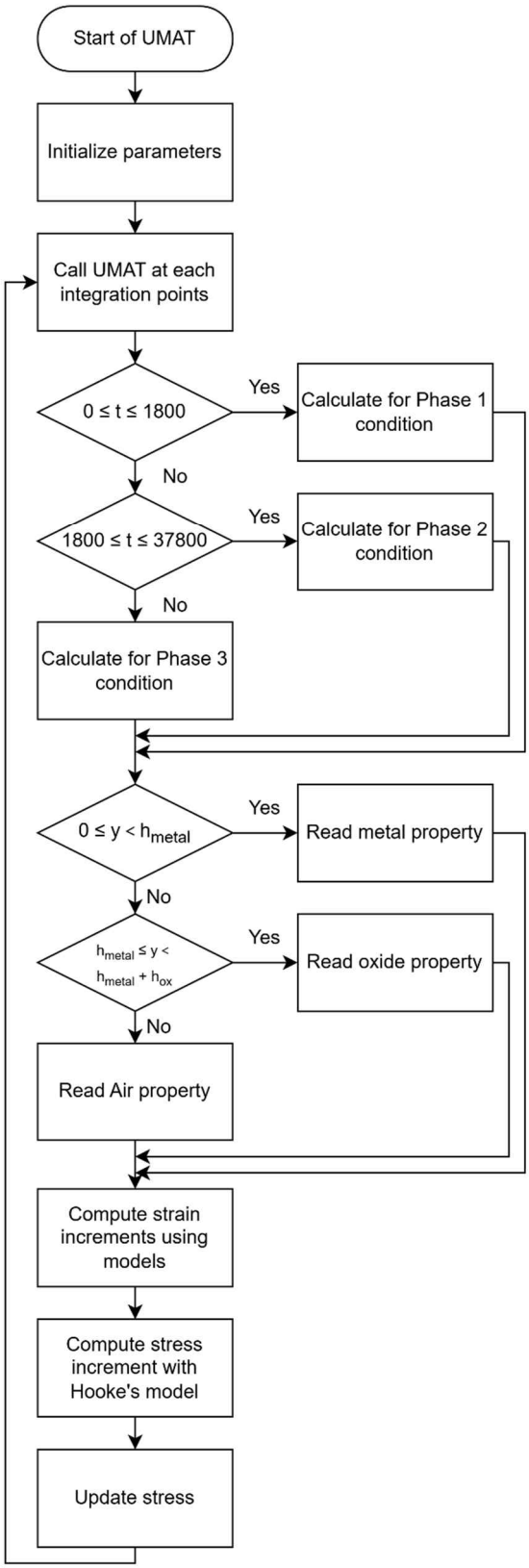

Fig. 3. Flowchart of UMAT implementation

We used common block function to track the deformed thickness, sharing this data across all integration points. This approach allows clear differentiation of the metal-oxide interface, resulting in more precise outcomes.

4. Conclusions

This study addresses the use of the finite element method (FEM) to predict stress distribution during high-temperature oxidation. This work is beneficial for predicting spatial stress distribution, particularly at the oxide-metal interface. Since damage often initiates at this interface, analyzing localized stress distributions may help improve predictions of material lifetime.

REFERENCES

[1] Strafford, K. N. "'Protective oxide scales and their breakdown'." *Materials Science and Technology* 14.11 (1998): 1200.
[2] Wang, Zhimao, et al. "Finite element analysis of stress evolution during the high temperature oxidation of Ni30Cr+ Cr2O3 systems." *Journal of Alloys and Compounds* 904 (2022): 164094.
[3] Tolpygo, V. K., J. R. Dryden, and D. R. Clarke. "Determination of the growth stress and strain in α-Al2O3 scales during the oxidation of Fe–22Cr–4.8 Al–0.3 Y alloy." *Acta Materialia* 46.3 (1998): 927-937.
[4] Panicaud, Benoît, et al. "Comparison of growth stress measurements with modelling in thin iron oxide films." *Applied surface science* 252.24 (2006): 8414-8420.
[5] Wang, Zhimao, et al. "Stress distribution in depth of NiCr+ Cr2O3 systems using high-energy synchrotron X-rays in transmission mode." *Journal of Alloys and Compounds* 875 (2021): 159958.
[6] Panicaud, Benoit, et al. "Mechanical features optimization for α-Cr2O3 oxide films growing on alloy NiCr30." *Computational Materials Science* 46.1 (2009): 42-48.